Real-time Navigation, Guidance, and Control of a UAV using Low-cost Sensors

Jong-Hyuk Kim, Stuart Wishart* and Salah Sukkarieh
Australian Centre for Field Robotics
University of Sydney, NSW 2006, Australia
Telephone: +61 (2) 9351 7154
Fax: +61 (2) 9351 7474
Email: {jhkim,salah}@acfr.usyd.edu.au
*BAE Systems, Australia
Email: {s.wishart}@acfr.usyd.edu.au

***Abstract*— Applying low-cost sensors for the Guidance, Navigation and Control (GNC) of an autonomous Uninhibited Aerial Vehicle (UAV) is an extremely challenging area. This paper presents the real-time results of applying a low-cost Inertial Measurement Unit (IMU) and Global Positioning System (GPS) receiver for the GNC. The INS/GPS navigation loop provides continuous and reliable navigation solutions to the guidance and flight control loop for autonomous flight. With additional air data and engine thrust data, the guidance loop computes the guidance demands to follow way-point scenarios. The flight control loop generates actuator signals for the control surfaces and thrust vector. The whole GNC algorithm was implemented within an embedded flight control computer. The real-time flight test results show that the vehicle can perform the autonomous flight reliably even under high maneuvering scenarios.**

***Index Terms*— Autonomous UAV, low cost sensors, Kalman filter, guidance and control, flight control system.**

I. Introduction

Over the recent years the use of low cost Uninhibited Aerial Vehicle (UAV) for civilian applications has evolved from imagination to actual implementation. Systems have been designed for fire monitoring, search and rescue, agriculture and mining. In order to become successful the cost of these systems has to be affordable to the civilian market, and although the cost/benefit ratio is still high, there have been significant strides in reducing this, mainly in the form of platform and sensor cost.

However, reduction in sensor cost also generally brings about a reduction in sensor accuracy and reliability. Coupled with the generally high mission dynamics that vehicles undertake within civilian aerospace due to the restricted mission areas, ensures that the design and implementation of these sensors is an extremely challenging area.

More importantly, the implementation of low cost sensors which are used for the Guidance, Navigation and Control (GNC) of the aerial vehicle is where most interest lies although little research is done. When applying a low cost Inertial Measurement Unit (IMU) there are still a number of challenges which the designer has to face. The main restrictions are the stability of the Inertial Navigation System (INS) degraded by the inertial sensor drifts. The quality and integrity of aiding sensors is also the crucial factor for the integrated system.

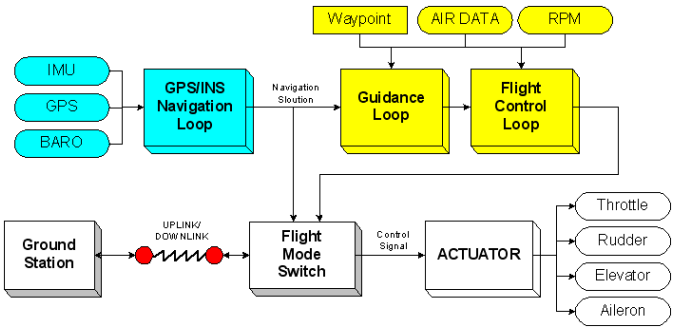

Fig. 1. The overall structure of navigation, guidance and control loop in UAV.

The Global Positioning System (GPS) can provide long-term stability with high accuracy. It also provides worldwide coverage in any weather condition. As a result lots of research have been done to optimally blend the GPS and INS [6][7][8]. Since the performance of the low cost GPS receiver can be easily degraded in high maneuvering environments, the quality and integrity of the GPS system becomes also a crucial factor. In case of GPS outage or fault conditions, the stand-alone INS quality then becomes the dominate factor. If the cost is a prohibitive factor in developing or buying an IMU, then improvements in algorithms, and/or fusing the navigation data with other sensors such as a barometer is required.

In this paper the authors present a low-cost navigation system which is successfully applied to the GNC of a UAV. Figure 1 depicts the overall GNC structure implemented in the Flight Control System (FCS). In remote operation mode, the remote pilot on the ground sends the control signals to the actuator via wireless uplink channel. The INS/GPS/Baro navigation loop downlinks the vehicle states to the ground station for vehicle state monitoring. When the autonomous mode is activated, the navigation solution is fed into the guidance and control loop and the onboard Flight Mode Switch (FMS) redirects the computed control outputs to the actuators.

The INS/GPS/Baro navigation loop makes use of a four-sample quaternion algorithm for the attitude update [2]. A complementary Kalman filter is designed with the errors in po-

sition, velocity and attitude being the filter states. It estimates the low-frequency errors of the INS by observing the GPS data with noises. In actual implementation, a U/D factorised filter is used in order to improve the numerical stability and computational efficiency [3][13]. Under high maneuverability, part of the GPS antenna can be blocked from the satellite signals which cause the receiver to operate in 2D height-fixed mode, hence to maximise the satellite visibility under these conditions, a second redundant receiver is installed and used.

The guidance loop generates the guidance commands from the vehicle states and the desired waypoint information. It computes required vehicle speed with respect to the air, height and bank angle. Then the flight control loop (or autopilot) generates actuator control signals to make the vehicle follow the guidance demands as well as to stabilise the vehicle. The control outputs are fed to the control surfaces, or aileron, elevator and rudder, and thrust vector [4][5].

The whole navigation, guidance and control software package was developed using the C++ class methodology. They are implemented and installed within a FCS which has a multitasking capability. The developed flight vehicle, MK3-Brumby, is a delta fixed wing platform with a pusher prop configuration. It can carry an extra sensor payload for different mission objectives. These sensors include radar, vision and laser; and hence the accuracy of the navigation loop is not only for control purposes but also for the accurate registration of landmarks which these mission sensors pick up. The real-time flight tests show that the navigation system can provide accurate and reliable 3D navigation solutions as well as to perform the guidance and control task reliable.

Section II will briefly describe the aircraft system including the flight platform, onboard systems, and ground system. Section III will provide the details of the low-cost sensors used in this work. Section IV will describe the navigation loop. Section V will detail the structure of the guidance and control loop. Section VI will present the result of a real-time autonomous flight test. Conclusions are then provided in Section VII.

II. Aircraft Systems

The physical aircraft system comprises of the flight platform, on-board systems, communication links, and ground station.

The flight platform, MK3-Brumby, is shown in figure 2. It is a delta fixed wing platform with a pusher prop configuration and is capable of flying at $100kts$ and up to $500m$. The platform can carry up to $11kg$ of additional mission sensors (the payload sensors are part of the flight platform). Figure 3 shows four UAVs built for the demonstration of cooperative data fusion amongst multiple vehicles [12].

The on-board systems consist of an FCS, FMS, vision system, scanning radar and/or laser system, and an air data system. The vision and radar systems are mission specific nodes and perform multi-target tracking, target registration and decentralised data fusion.

The air-to-air/air-to-ground communication links are established for the decentralised fusion purposes, remote control operation, differential GPS data uplink, and telemetry data.

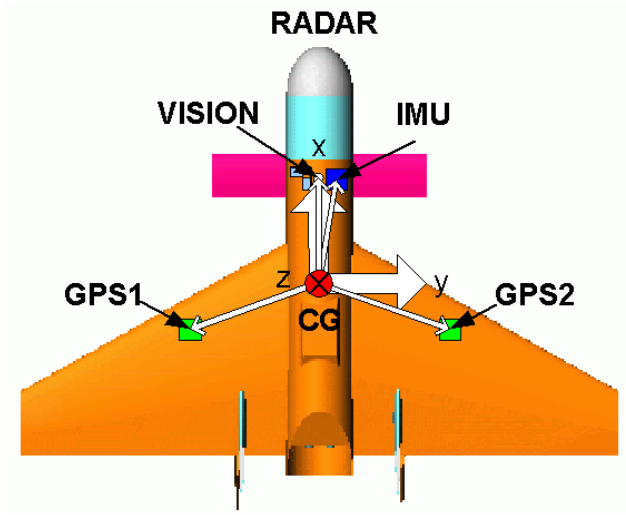

Fig. 2. The location of onboard sensors in the Brumby MK-3 UAV. It is equipped with IMU, GPS, vision camera, radar scanner, air data system, and flight electronics

Fig. 3. The four flight vehicles: MK3-Brumby. Four sets of identical GNC modules are installed on the vehicles with different mission load.

The ground station consists of a DGPS base station, weather station, hand-held controller, and monitoring computer. Additional mission computers performs the monitoring of the mission objectives.

III. Low-cost Sensors

The Inertial Measurement Unit (IMU) is an Inertial Science ISIS unit. Figure 4 shows the IMU installed in the fuselage of the vehicle. It is a short-range tactical grade IMU with three voltage resonant gyros and three accelerometers. It has a gyro bias repeatability within $0.01°/s$ and accelerometer bias repeatability within $1mg$. The IMU has very small physical dimension and consumes only 5 watts of power. The unit can provide inertial data from $100Hz$ to $400Hz$ through an RS422 serial interface. The resolution of the gyro is too low to detect the earth rotation rate and the self-azimuth alignment can not be performed for initialisation. In this work, the initial heading is uplinked from the ground station. The IMU makes use of an internal temperature lookup table for the temperature compensation. However, in field tests, the turn-on bias was not removed effectively so the calibration process was performed before starting the navigation. This was performed using a tilt sensor as shown in the upper right part on figure 4.

The GPS receiver is the BAE Systems $Allstar^{TM}$ receiver. Two GPS cards are stacked on the FCC as shown in figure 4. Their antennas are installed on each of the wings as shown in figure 5. The wing frame was made of fiber glass and the GPS signal loss was negligible. The master GPS receiver

provides navigation solutions to the Kalman filter. The slave receiver provides redundant navigation solution as well as the raw measurement data for the purpose of GPS attitude determination which is not implemented yet.

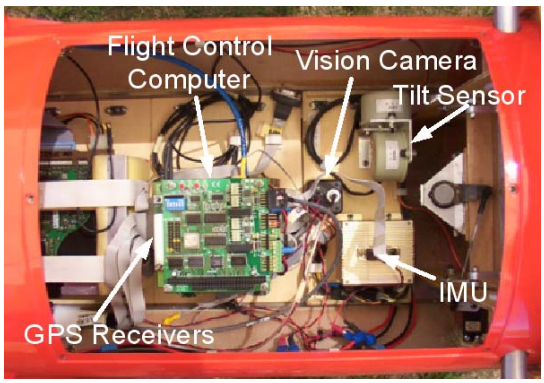

Fig. 4. A view from the front hatch of the vehicle. A low-cost IMU is installed (lower right) next to the vision camera pointing downwards and a tilt sensor (upper right). Two GPS receivers are stacked on the flight control computer. The sensors are connected to the flight control computer via serial and parallel lines.

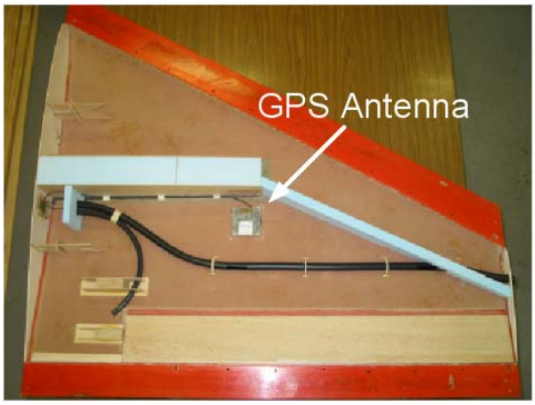

Fig. 5. A view of the GPS antenna installed inside the wing of the vehicle. Two antennas are installed on both of the wings to provide redundancy.

The air data system is implemented by using a $FlexIO^{TM}$ card developed by the University of Sydney as shown in figure 6. It is a multi-purpose A/D (Analog to Digital) and D/A (Digital to Analog) card which can sample various analog signals such as air pressure, temperature, engine RPM, battery current and voltage. The sampled data are sent to the FCS via RS232 serial interface and FCS downlinks them to the ground station for vehicle monitoring. The measured air data is used in the guidance and control loop and the baro-altimeter data is used to stabilise the vertical axis of the INS.

IV. Navigation Loop

The navigation loop plays a key role in aircraft system. Its navigation outputs are used in guidance and control and affect the performance of target registration and picture compilation tasks. It also has to provide precise timing synchronisation to other sensor nodes.

The core of the navigation loop is the strapdown INS and the Kalman filter. The strapdown INS provides continuous and

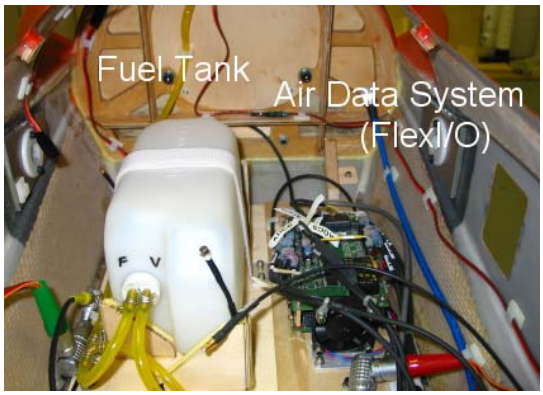

Fig. 6. A view from the rear hatch of the vehicle. The air data system can be seen next to the fuel tank. It is implemented using a FlexIO card which can be configured in multi-purpose data sampling.

reliable position, velocity and attitude with sufficiently high rates. The Kalman filter estimates the navigation errors by blending the GPS observation or baro-altimeter data running as a background task.

A. Inertial Navigation

The INS is mechanised in an earth-fixed tangent frame as shown in figure 7. It computes position, velocity and attitude of the vehicle with respect to the reference frame by numerical integration of the accelerations and angular rates. In this mechanisation scheme, the reference frame is assumed as a non-rotating inertial frame. The short mission flight time and the frequent GPS corrections makes this assumption valid without significant performance degradations in most of the local terrestrial navigators. If the INS should perform long-range missions without GPS corrections, the INS will require a more precise mechanisation scheme to remove systematic errors like frame rotation effect and coriolis force. In this earth-fixed tangent frame mechanisation, the coriolis and transport rates term are not calculated. The navigation outputs are in MGA (Map Grid Australia) coordinate format instead of WGS-84 coordinate as it is convenient to exchange the vehicle states and relative target observations between multiple UAVs.

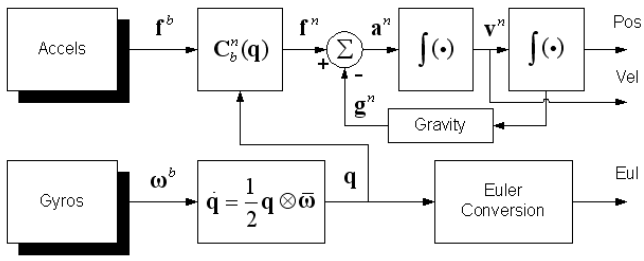

Fig. 7. The INS mechanisation in the earth-fixed tnagent frame.

B. Fusion Kalman Filter

The fusion Kalman filter is the heart of the navigation system. In a low-cost system the IMU errors like bias, scale factor error and random walk noise dominate the INS error

growth. These INS errors typically show low dynamics and its models have been well developed [1]. The INS error model in earth-fixed tangent frame is used in this paper [11].

Figure 8 shows the complementary filter structure that deals with the INS error state instead of the total vehicle states using the INS error model. Since the INS error has low frequency dynamics, the filter can run in relatively low sample rates with lower priority. When the external aiding information from GPS or baro-altimeter is available, a measurement residual is generated by subtracting the actual measurement from the INS predicted measurement. The resulting residual contains the INS error as well as the measurement error. The measurement error typically has high-frequency noise and can be modelled as white (or broadband white) noise process. The Kalman filter suppresses this high-frequency noise and estimates the INS error by the low-pass filtering nature. If the measurement error contains additional dynamic error, this should be properly modelled inside the filter [3].

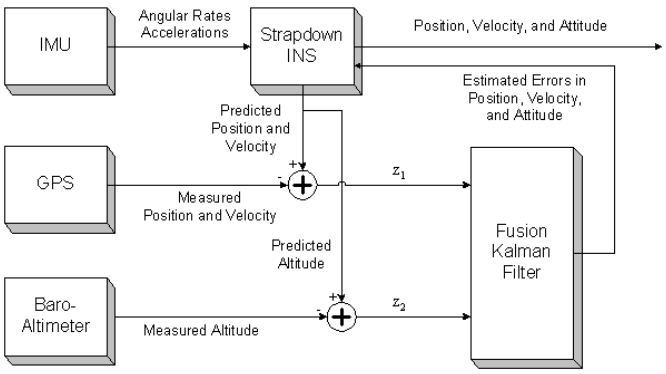

Fig. 8. The complementary INS/GPS/Baro Kalman filter.

V. Guidance and Flight Control Loop

The guidance loop forms an outer control loop in autonomous mode. It computes guidance demands to force the vehicle to follow the desired way-point. The flight control (or autopilot) loop forms the inner control loop and it generates the actual control signals to follow the guidance objectives as well as to stabilise the vehicle attitude and its rate.

A. Guidance

The guidance loop generates the guidance demmands from the current vehicle states and the next waypoint information. The guidance demands are desired vehicle speed with respect to the air, desired height and bank angle as shown in figure 9. If the autonomous mode is activated, it selects the appropriate next waypoint depending upon the guidance state. Then it decides if the waypoint has been intercepted or missed. If it is not intercepted it determines the Line Of Sight (LOS) angles and LOS rates to the next waypoint. Based on this information it computes the lateral acceleration required to intercept the next waypoint and converts this acceleration to the desired bank angle with a set of additional guidance demands: airspeed and height [4]. The guidance loop implemented in this work updates its guidance demands every 10Hz.

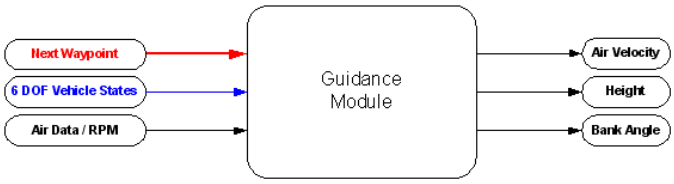

Fig. 9. The guidance structure.

B. Flight Control

The flight control loop controls the vehicle's attitude and attitude rates as well as the vehicle speed with respect to the air. The block diagram of the control loop is shown in figure 10. It performs speed control, height and height rate control, bank angle control, heading control, turn compensation and elevation control by using the guidance demands and measured vehicle states. It generates actuator signals for the engine throttle, rudder, elevator, and aileron. In this work, the control loop generates the control signals every 50Hz which is limited by the bandwidth of the electric servo actuators. The control loop is the most time critical task in autonomous flight so it is allocated to the highest priority inside the FCS. Most of the guidance and control algorithms were verified and tested using the Hardware-In-The-Loop (HWIL) simulator which uses the vehicle model and simulated sensor data in the laboratory. However the true vehicle model and control action to the vehicle can only be verified through real-time flight tests.

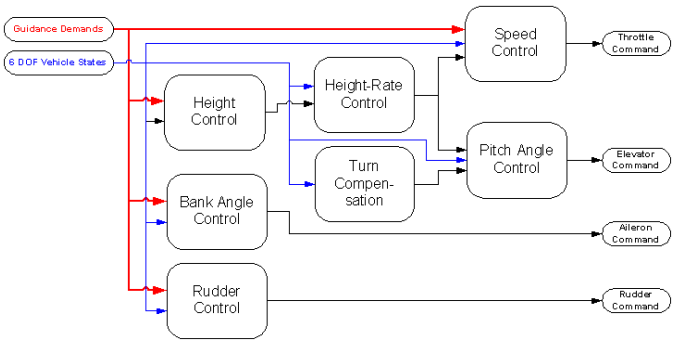

Fig. 10. The control structure.

VI. Real-time Results

Several real-time autonomous flight tests were performed at the test site of the University of Sydney. To evaluate the navigation performance, a more precise navigation system which usually has an order of accuracy is required as a reference system. However, due to the limited payload capacity of the UAV, this was not adopted. Instead, the covariance and innovation data from the fusion filter were used to evaluate the performance and the filter consistency.

A flight test was performed on April 17, 2003. The purpose of this test was to verify the real-time autonomous flight with different sets of waypoint scenarios. The total flight time was $25min$ and the desired flight height in autonomous mode was set to $328ft$ above the ground and the desired air speed was set to $80kts$.

The full flight trajectory is shown in figure 11. The blue solid line is the real-time estimated positions and the red dotted line is the GPS indicated position. Except take-off and landing the vehicle flied in autonomous mode. Figure 12 depicts the vehicle trajectory from the take-off in remote control mode until the activation of autonomous mode. Figure 13 shows the trajectory in autonomous mode with 6 waypoints. During the first six rounds, the waypoints are activated in CCW sequences with some transition sequences. After the seventh round the way points are changed to CW sequences. The former scenario requires higher vehicle maneuvers than the latter. This can be seen in the guidance response in figure 15 which show larger overshoots in measured vehicle speed and height as well as in bank angle. After performing the last scenario, the vehicle mode is changed to remote mode to prepare the landing approach and is returned to the ground station as shown in figure 14.

During the test the number of GPS satellites changed from eight to four during banking. The estimated vehicle 1σ uncertainties in position were maintained within $2m$ in three axes as shown in figure 16. The attitude uncertainties are shown in figure 17 where the roll and pitch uncertainties are maintained under $0.4°$ and the heading is under $0.8°$.

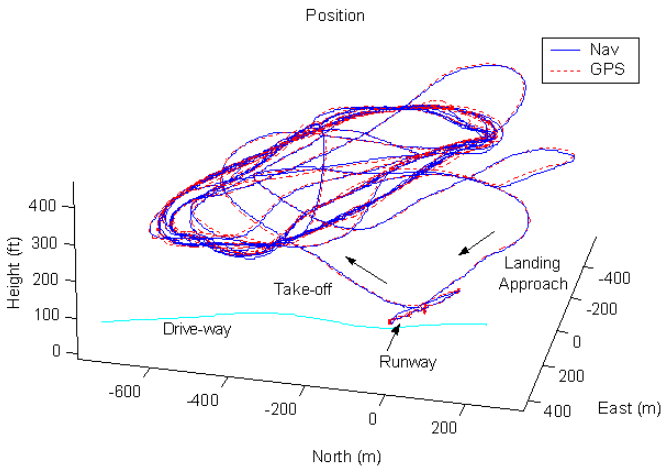

Fig. 11. Real-time estimated 3D trajectory. the vehicle took off and landed in remote control mode. The autonomous mode was activated after the first round and performed several scenarios which has different sequences of waypoints.

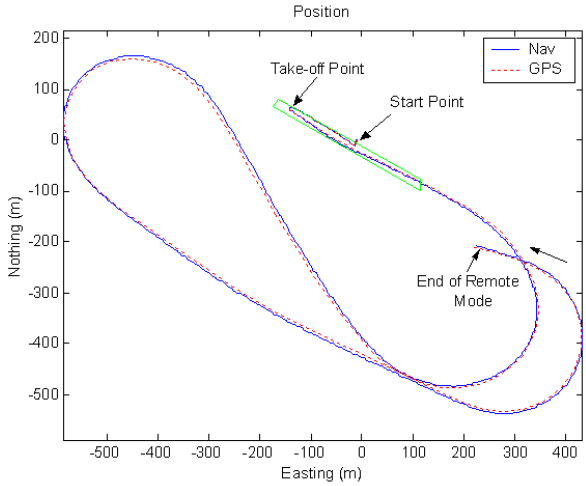

Fig. 12. The vehicle takes off in remote control mode.

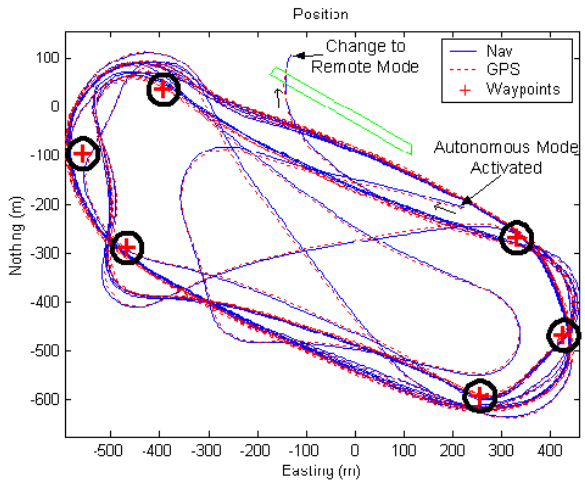

Fig. 13. The autonomous mode is activated after the take-off. The guidance loop uses the uplinked waypoints information to find out the next destination. Various combinations of waypoint sequences are applied which requires different dynamics on the vehicle.

VII. Conclusions

This paper presents the real-time implementation and result of the navigation, guidance, and control of UAV using low-cost sensors. A low tactical grade IMU is used for the inertial navigation and two low-cost commercial GPS receivers are used to estimate and correct the INS error. The air data system is built using a customised analog/digital conversion card. It provides air pressures, temperature and engine control signal for the guidance and control loop. The GNC algorithm was developed in C++ methodology and implemented in an embedded computer. Real-time autonomous flight tests shows reliable and accurate GNC performances with several way-point scenarios. With the low-cost aircraft platform and GNC module, the FCS becomes a modular and powerful autonomous system. This system is planned to be used for decentralised data fusion between multiple UAVs. The future work is to make this system to be fully autonomous which does not rely on the external GPS aiding signal by exploring the unknown environments and map building process.

Acknowledgements

The authors wish to thank BAE Systems for their support in providing funding and systems engineering towards this project.

References

[1] D.G. Meskin and I.Y. Bar-Itzhack, "Unified Approach to Inertial Navigation System Error Modeling," *Journal of Guidance, Control, and Dynamics*, vol. 15, no. 3, pp. 648–653, May-June 1992.

[2] P. G. Savage, "Strapdown Inertial Navigation Integration Algorithm Desogn Part I: Attitude Algorithms," *Journal of Dynamic Systems, Measurement and Control*, vol. 21, no. 1, pp. 19–28, January-February 1998.

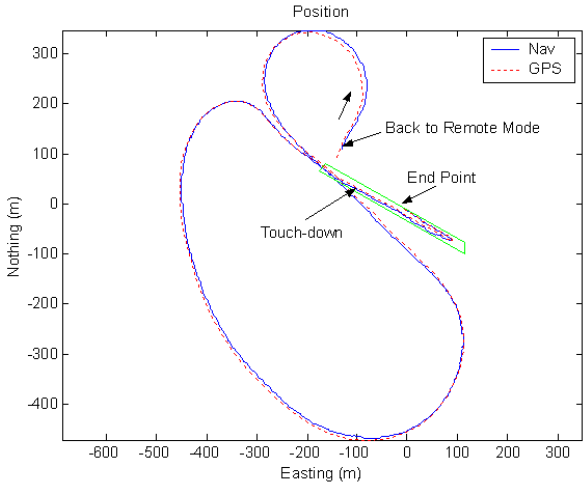

Fig. 14. The vehicle is back to remote control mode to prepare the landing approach.

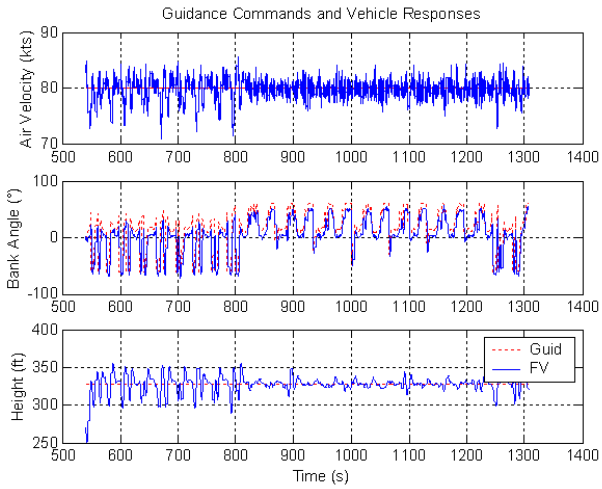

Fig. 15. The vehicle responses to the guidance demands in autonomous mode. The desired air velocity was set to 80 knts and desired altitude above the ground was set to 328 ft. The desired bank angle was calculated from the current vehicle state and the next waypoint. During the first six rounds, the vehicle undergoes more severe dynamics by controlling the sequence of waypoints.

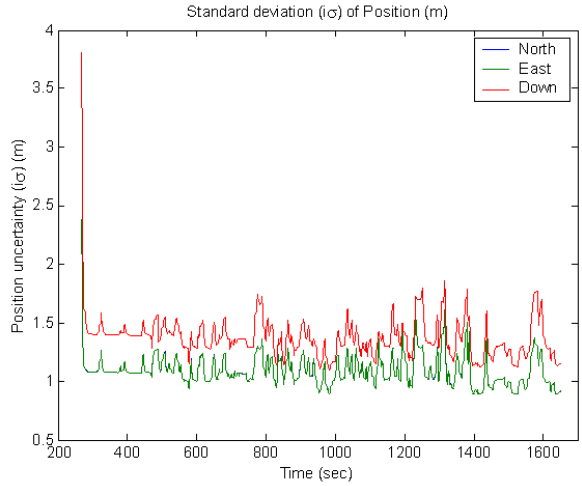

Fig. 16. The evolution of the vehicle 1σ uncertainty in position.

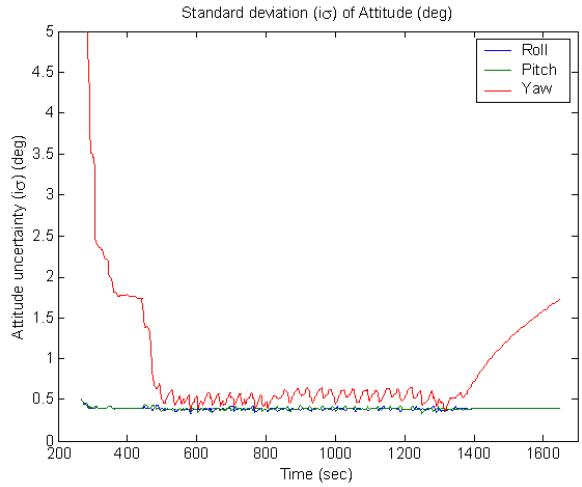

Fig. 17. The evolution of the vehicle 1σ uncertainty in attitude.

[3] M. Grewal and A. Andrew, *Kalman Filtering - Theory and Practice*. Prentice-Hall, Inc., 1993.

[4] B.L. Stevens, F.L. Lewis, *Aircraft Control and Simulation*, John Wiley and Sons, Inc., 1992.

[5] Skogestad, Postlethwaite, *Multivariable Feedback Design*, John Wiley and Sons, Inc., 1997.

[6] A. H. Lewantowicz. Architectures and GPS/INS Integration: Impact on Mission Accomplishment. In *IEEE Position, Location and Navigation Symposium*, pages 284–289, 1992.

[7] S. Snyder, B. Schipper, L. Vallot, N. Parker, and C. Spitzer. Differential GPS/Inertial Navigation Approach/Landing: Flight Test Results. In *IEEE Transactions on Aerospace and Electronic Systems Magazine*, pages 3–11, 1992.

[8] R.L. Greenspan. GPS and Inertial Navigation. In *American Institute of Aeronautics and Astronautics*, 1996.

[9] R.E. Phillips and G.T. Schmidt. GPS/INS Integration. In *Advisory Group for Aerospace Research and Development (AGARD)*, Lecture series 207:9.1–9.10, 1996.

[10] S. Sukkarieh, E.M. Nebot, and H. Durrant-Whyte. A High Integrity INS/GPS Navigation Loop for Autonomous Land Vehicle Applications. In *IEEE Transactions on Automatic Control*, 15:572–578, June 1999.

[11] S. Sukkarieh, "Aided Inertial Navigation Systems for Autonomous Land Vehicles," PhD thesis', Australian Centre for Field Robotics, The University of Sydney, 1999.

[12] S. Sukkarieh, A. Goktogan, J. Kim, E. Nettleton, J. Randle, M. Ridley, S. Wishart, and H. Durrant-Whyte, "Cooperative Data Fusion Amongst Multiple Uninhabited Air Vehicles," in *International Conference on Service and Experimental Robotics*, Italy, 2002.

[13] J.H. Kim and S. Sukkarieh. Flight Test Results of a GPS/INS Navigation Loop for an Autonomous Unmanned Aerial Vehicle (UAV). In *Proceedings of the 15th International Technical Meeting of the Satellite Division of the Institute of Navigation*, pages 510–517, September, OR, USA, 2002.